

Electron-spin-lattice relaxation in amorphous silicon and germanium

M. Stutzmann and D. K. Biegelsen

Xerox Palo Alto Research Center, Palo Alto, California 94304

(Received 21 June 1983)

Electron-spin-lattice relaxation times have been measured using adiabatic-passage techniques in doped and undoped *a*-Si:H and *a*-Ge:H. When scaled by the square of the atomic spin-orbit coupling constants, the magnitudes of the relaxation times are found to be surprisingly similar. The temperature dependence of the dangling bonds and band-tail states in all cases shows a nearly quadratic behavior to temperatures far below the Debye temperature. The results are shown to be consistent with relaxation via two-level systems (TLS's). The TLS's make transitions between levels by phonon-assisted tunneling and flip spins by modulating the spin-orbit interaction. Hydrogen evolution studies allow us to vary the TLS distribution and show that the TLS density of states is related to the degree of departure of the network from its thermal-equilibrium value.

INTRODUCTION

Electron-spin resonance (ESR) has proved to be a powerful tool for the characterization of electronic states in the gap of amorphous semiconductors. In the hydrogenated tetrahedrally bonded amorphous semiconductors (e.g., *a*-Si:H, *a*-Ge:H, and *a*-C:H) spin is an excellent marker. The paramagnetic states, either in equilibrium or nonequilibrium, are generally localized and essentially magnetically isolated. Any particular site has a corresponding set of energy levels demarcating the various states of electron occupation. ESR, which is sensitive to

unpaired spins, then probes an ensemble of states lying within an energy band (approximately the positive effective correlation energy, U_{eff} below the equilibrium or quasi-Fermi-level—as indicated in Fig. 1.

In *a*-Si:H it has been shown that, as E_F is moved by doping or optical excitation, three distinct ESR signatures are observed corresponding to singly occupied conduction-band-tail states, valence-band-tail states, and dangling bonds.¹ It has also been found that in *a*-Ge:H, after accounting for a scaling of the g value by a factor approximately equal to the ratio of the atomic spin-orbit coupling factors, $\lambda_{\text{Ge}}/\lambda_{\text{Si}}$, the ESR signatures, i.e., g values and low-temperature linewidths, are basically the same.²

When the spin temperature, T_s , of a spin system is driven away from its equilibrium value, the temperature generally relaxes with a characteristic time, T_1 , to equalize with the temperature of the network. This spin-lattice relaxation time depends on the ground state of the electronic center and excited states to which it is coupled by temporal fluctuations of the network or neighboring spins.³ In crystals the network fluctuations are phonons. In many amorphous materials, "tunneling modes" or "two-level systems" (TLS) exist as a separate set of excitations.^{4,5} Experimental measurements of T_1 thus are useful in learning about the gap states and the structural excitations. Results of studies of the temperature dependence of T_1 for dangling bonds in undoped hydrogenated amorphous silicon, *a*-Si:H, have been published previously.^{6,7} In this paper we present measurements of T_1 as a function of temperature, T , for the three characteristic electronic states in both *a*-Si:H and *a*-Ge:H. The results are then used to elucidate the mechanisms of spin-lattice coupling.

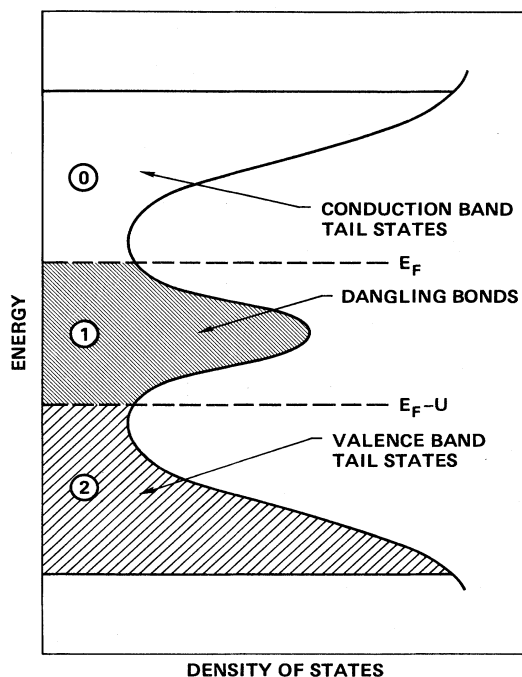


FIG. 1. Schematic density of states of *a*-Si:H and *a*-Ge:H. The states between E_F and $E_F - U$ are single occupied and paramagnetic. Those below $E_F - U$, marked 2, are doubly occupied and spin paired.

EXPERIMENT

T_1 was obtained by the technique of periodic adiabatic passage as described by Ammerlaan and van der Wiel.⁸ (The lowest-temperature T_1 values in phosphorus-doped *a*-Si:H were obtained by single-passage time-domain averaging.) The X-band ESR dispersion signal 90° out of

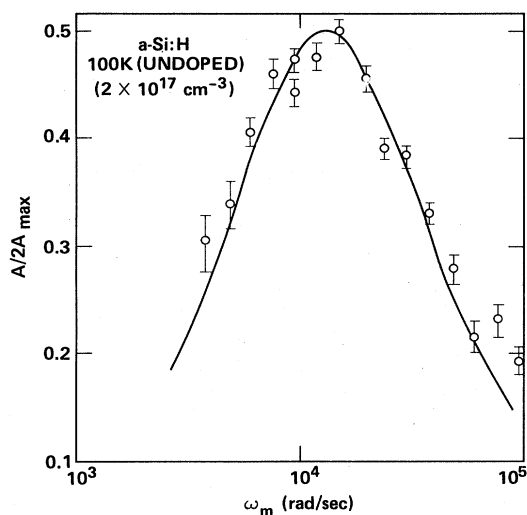


FIG. 2. Normalized-passage signal amplitude, $A/2A_{\max}$, vs modulation frequency, ω_m , for undoped $a\text{-Si:H}$ at 100 K. The solid line is the theoretical curve for single T_1 .

phase with the field modulation is observed. When the passage conditions are adiabatic ($\omega_m H_m \ll \gamma H_1^2$, where ω_m and H_m are the modulation frequency and amplitude, respectively, γ is the gyromagnetic ratio, and H_1 is the microwave magnetic field), the signal amplitude varies as $T^{-1} \omega_m T_1(T) \{1 + \omega_m^2 [T_1(T)]^2\}^{-1/2}$, a Lorentzian which peaks at $\omega_m T_1 = 1$. $T_1(T)$ can thus be derived by varying ω_m at fixed T , or vice versa. In fact, multiple runs at various ω_m values were made for each sample. Figure 2 is a typical example for the variation of the signal amplitude with ω_m for fixed T . The solid curve shows the theoretical $x/(1+x^2)$ dependence for a single T_1 . In the case of a distribution of T_1 's the experimental data should show a somewhat larger full width at half maximum. The results (where measurable) are consistent with a narrow distribution in T_1 ($\Delta T_1/T_1 < 50\%$). Furthermore, the peak passage signal ($\omega_m T_1 = 1$) very nearly follows a Curie temperature dependence, indicating again that the relaxation of most of the spin population is being observed. This measurement is in fact quite difficult because the passage conditions are not identical at each temperature. For the dangling bonds in $a\text{-Si:H}$ the passage signal actually follows a T^{-x} law, where $x = 0.6 \pm 0.1$. We thus expect that at low temperatures a wider distribution in T_1 exists. The absolute uncertainty in the T_1 measurements is approximately a factor of 2. However, relative errors are less than 10%. The spin-spin relaxation time, T_2 , can be determined from saturation measurements when T_1 is known. (Saturation measurements could be made down to 20 K in $a\text{-Ge:H}$ without running into passage effects. Similar studies could not be made to such low temperatures in $a\text{-Si:H}$.) The usual assumption was confirmed that the lines at low spin densities are inhomogeneously broadened. In fact, the dynamic T_2 is limited by T_1 .

Samples were deposited from an rf plasma consisting of pure or doped SiH_4 or GeH_4 . The conditions, as described elsewhere, result in microscopically homogeneous materi-

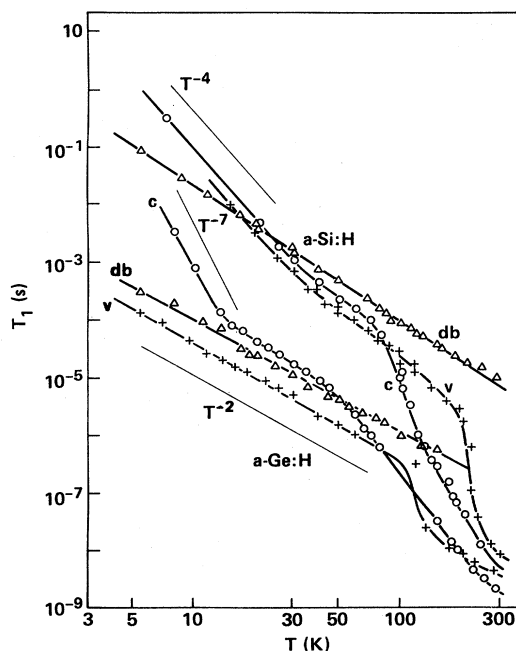


FIG. 3. T_1 vs temperature for the dangling bonds, conduction-band-tail states, and valence-band-tail states in $a\text{-Si:H}$ and $a\text{-Ge:H}$.

al, free of observable microstructure.⁹ The films were deposited on metal-foil substrates, removed, and ~ 100 mg of the flakes were collected into quartz tubes having ~ 3 -mm inside diameter. A calibrated silicon diode inserted into the open-ended tube was used to monitor the sample temperature. Samples were cooled between 5 and 300 K ($\pm 3\%$) by a He-gas-flow cryostat. Cavity Q changes were found to be negligible.

In Fig. 3 the T_1 data for $a\text{-Ge:H}$ and $a\text{-Si:H}$ are plotted versus temperature. The $a\text{-Ge:H}$ samples generally have

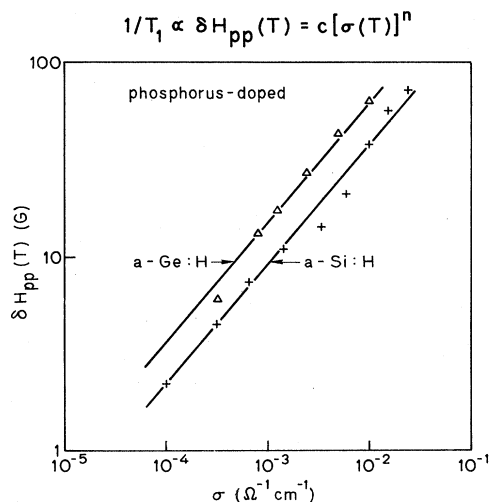


FIG. 4. Power-law relationship between the excess, temperature-dependent linewidth and conductivity in two $a\text{-Si:H:P}$ and $a\text{-Ge:H:P}$ samples.

shorter lifetimes than *a*-Si:H. It also seems evident that there are three temperature regimes: (a) a rapid decrease in T_1 at high temperatures for band-tail states, (b) an approximately T^{-2} behavior for all states, and (c) a stronger T dependence, again for the band-tail states, at low temperatures. The reduction in relaxation times at high temperatures arises from the proximity of band-tail states to the high density of extended states beyond the mobility edges. Thermal excitation and/or interactions with thermally excited carriers lead to rapid spin flipping and lifetime broadening of the resonance lines.¹⁰ This is demonstrated in Fig. 4, where the power-law relation between incremental linewidth (increase in width beyond the low-temperature value) and conductivity at various temperatures is shown for two phosphorus-doped samples. In this regime, the excess linewidth is approximately $(\gamma T_1)^{-1}$. The dangling-bond energy levels, on the other

hand, lie much deeper in the band gap and, in equilibrium, show no signs of such coupling. (However, when an undoped sample is irradiated with band-gap light, T_1 does decrease due to nonradiative recombination at the dangling bonds.)

A considerable simplification of the data follows if we again scale the magnetic properties using the atomic spin-orbit coupling constants ($\lambda_{\text{Si}}=0.019$ eV, $\lambda_{\text{Ge}}=0.138$ eV). If, and only if, the relaxation results from a dynamic network distortion modifying the orbit, the spin-orbit coupling term in the perturbing Hamiltonian is linear in λ , and the spin-flip transition probability, T_1^{-1} , is proportional to the square of the coupling matrix element, and therefore varies as λ^2 . In Figs. 5(a)–5(c) we therefore plot $T_1\lambda^2$ for the three centers. To the extent that phonons mediate the relaxation process, the temperature dependence can be scaled by the Debye temperature, Θ_D .

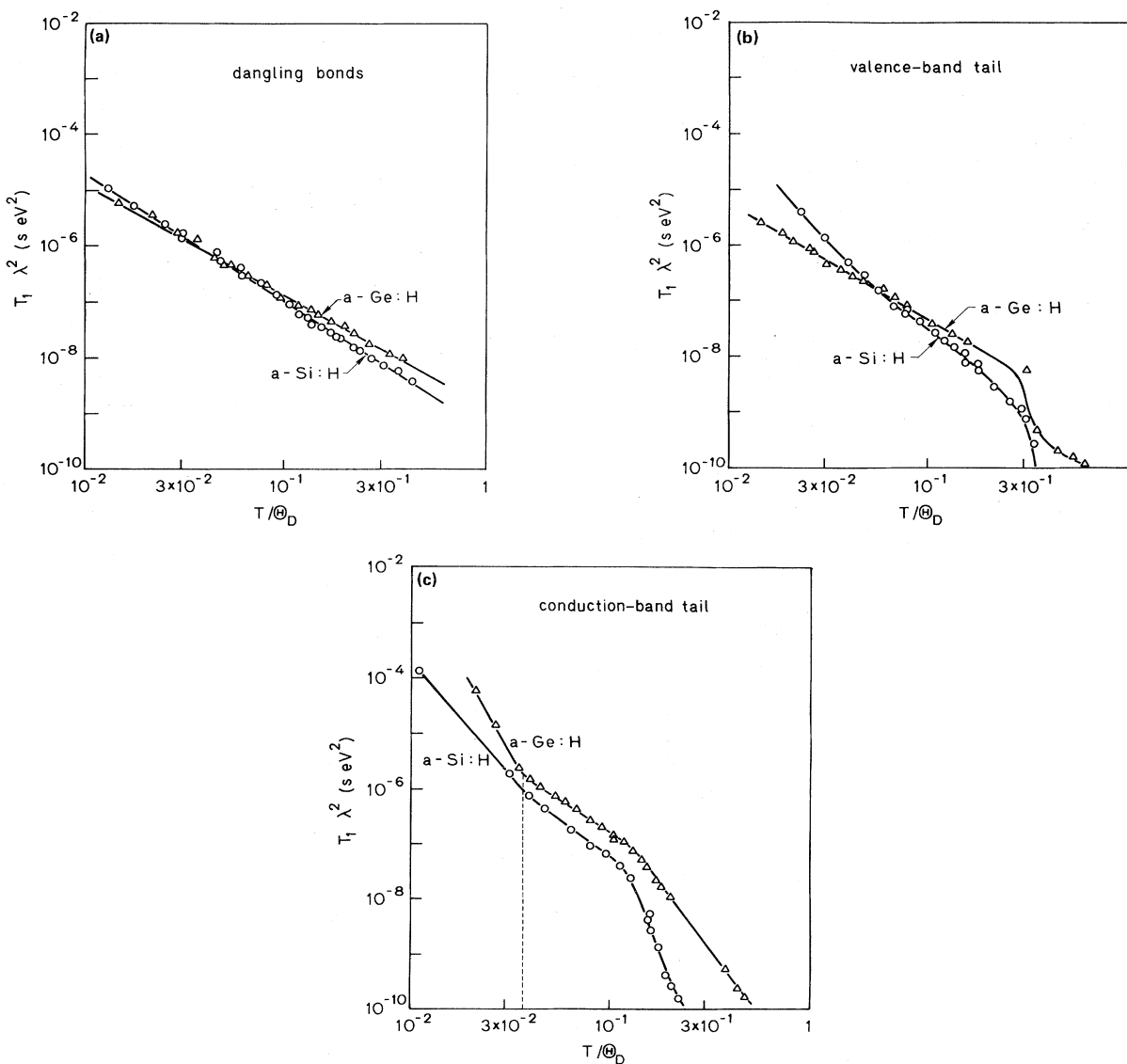


FIG. 5. T_1 , scaled by the square of the atomic spin-orbit coupling constants, vs T , scaled by the Debye temperature: (a) dangling bonds; (b) valence-band-tail states; (c) conduction-band-tail states in *a*-Si:H and *a*-Ge:H.

($\Theta_D^{\text{Si}}=647$ K and $\Theta_D^{\text{Ge}}=378$ K; $\Theta_D^{\text{Si}}/\Theta_D^{\text{Ge}}=1.7$). In Fig. 5 we have therefore chosen tentatively to scale the temperature axis. Values of T_1 for the dangling bonds [Fig. 5(a)] are seen to reduce, within a factor of 2, to the same absolute values for *a*-Si:H and *a*-Ge:H. A single, approximately quadratic, power-law T^{-p} ($p_{\text{Si}}=2.3$ and $p_{\text{Ge}}=2.0$) holds for the dangling bonds throughout the temperature range measured. Results for the band-tail states are shown in Figs. 5(b) and 5(c). Again a quadratic regime can be inferred, and approximately the same absolute values of T_1 occur. Below $T/\Theta_D \simeq 4 \times 10^{-2}$ the relaxation time for the conduction-band-tail states takes on a stronger temperature dependence. Apparently this is also the case for the valence-band-tail states in *a*-Si:H.

For clarity in the development of this paper we stop the presentation of experimental results temporarily here. It is clear at this point that, independent of the nature of the network fluctuations driving the spin-lattice relaxation, for the λ^2 scaling to be correct, the spin-orbit coupling must be the magnetic coupling mechanism.

DISCUSSION

The most important unexplained results regarding T_1 which have been presented thus far are the quadratic temperature dependence to $T/\Theta_D \ll 1$, the nearly constant value of $T_1 \lambda^2$ for the six characteristic states, and the superquadratic behavior for the band-tail states below $T/\Theta_D \sim 4 \times 10^{-2}$.

When a spin flips by emitting or absorbing a single lattice excitation, only those excitations which are equal in energy to the Zeeman splitting E_Z are effective for the relaxation. At all but very low temperatures, two-phonon Raman processes usually dominate the relaxation of spins in crystalline lattices, because all thermally occupied phonon modes (with $\hbar\Omega \geq E_Z$) can contribute as long as $\hbar\Omega_1 - \hbar\Omega_2 = E_Z$. At temperatures well below the Debye temperature this process leads to $T_1^{-1} \propto T^m$ where $m \sim 7$ (depending on the details of the spin system and relaxation). Only for $T/\Theta_D \geq 0.5$ does T_1^{-1} approach T^2 . The results shown in Fig. 5 thus clearly indicate that a simple two-phonon process is invalid here.

It is usually the case that relaxation times in amorphous materials are shorter than in their crystalline analogs.¹¹ The cause is thought to be the presence of an excess density of states associated with an excitation of localized TLS. The presence of TLS in *a*-Si:H has been deduced from Raman studies of low-energy excitations¹² and a T -linear specific heat at least as large as that in SiO₂.¹³

From the results presented above indicating a single T_1 (Fig. 2) for the isolated spins, we are led to conclude that the relaxation path is homogeneous. Therefore, because spin diffusion is ruled out ($T_2 = T_1$), diffusion of excitation energy within the TLS must be rapid compared with the TLS-bath relaxation time. Measurements of spectral diffusion within the TLS ensemble in similar systems¹⁴ indicate that this assumption is reasonable.

The density of states $n(E)$ of the TLS is larger than the phonon density of states for $T \leq 20$ K.¹⁵ It is generally assumed that $n_{\text{TLS}}(E) \propto E^\epsilon$ where ϵ is between 0 and 1. Because the phonon density of states $\rho_{\text{ph}}(\omega) \propto \omega^2$ and because

phonons are bosons whereas TLS are effectively fermions, the number of phonons above 20 K greatly exceeds the number of thermally excited TLS. However, because for the dangling bonds, as an example, a single power law fits $T_1(T)$ from 5 to 300 K, it is apparently implied by the experimental results that the TLS dominate the relaxation at least up to room temperature. Therefore, the coupling between localized spins and (localized) TLS is much stronger than between spins and long-wavelength phonons. This seems plausible in that the orbital angular momentum of any given localized electronic state is not greatly affected by a long-wavelength acoustic phonon (the strain is distributed), whereas it can be appreciably different in the two atomic configurations of a TLS. That is, although the total energy of the two states of the TLS are nearly equal, the electronic configuration at a specific site can differ greatly. Thus, although the TLS may make a small contribution to the specific heat (relative to the phonons), they can be particularly effective in relaxing localized spins.

The three processes which are candidates for the relaxation mechanism are a two-TLS and a TLS-phonon ‘‘Raman’’ process and a single TLS resonant relaxation process. The one and two TLS mechanisms give a $T^{1+\epsilon}$ behavior for $\Delta_0 < k_B T < E_m$, where Δ_0 and E_m are the minimum and maximum energy limits of the TLS distribution and ϵ is the TLS density-of-states exponent.¹¹ The TLS-phonon Raman process leads to a spin-lattice relaxation rate proportional to the average TLS relaxation rate,¹⁶ and is given by

$$T_1^{-1}(T) \propto M_{ST}^2 M_{TP}^2 \int_0^\infty E \operatorname{csch}(2E/k_B T) n(E) dE, \quad (1)$$

where M_{ST} and M_{TP} are the matrix elements coupling the TLS levels with the spin states and phonons, respectively, and $2E$ is the level splitting of a particular TLS. For $\Delta_0 \ll k_B T \ll E_m$, as indicated for these experiments, and assuming that the matrix elements are independent of TLS and phonon energy and that $n(E) = n_T = N_T / (E_m - \Delta_0)$ (i.e., $\epsilon = 0$) (where n_T is the constant TLS density of states and N_T is the total number of TLS),

$$T_1^{-1}(T) \propto n_T M_{ST}^2 M_{TP}^2 (k_B T)^2. \quad (2)$$

(The result of Ref. 16 is in error in predicting a linear- T behavior for these assumptions.) For $\epsilon \neq 0$, T_1^{-1} varies approximately as $T^{2+\epsilon}$. Because ϵ is usually estimated to be near zero, the TLS-phonon process seems to be the spin-lattice relaxation channel. The microscopic details of the process are clearly still ill defined and more work is in progress to develop a more precise understanding. What we do know now is that phonon-assisted tunneling modulates the orbital angular momentum of the localized electronic states to which the spins couple.

We do not yet know the origin of the superquadratic temperature regime of the band-tail states. This difference may be related to the decreased localization of these states.

We now address the issue of the origin of the TLS in these materials by observing $T_1(T)$ in related samples. To probe the role of hydrogen in the relaxation, a deuterated sample was prepared. In Fig. 6 an undoped *a*-Si:D sample

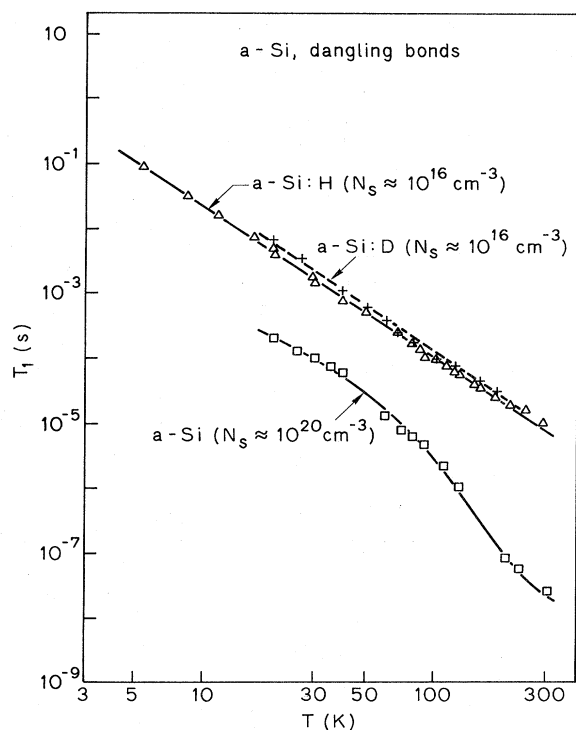


FIG. 6. $T_1(T)$ for otherwise equivalent samples of undoped a -Si:D and a -Si:H, and $T_1(T)$ for an unhydrogenated a -Si sample deposited by electron-beam evaporation.

grown from SiD_4 is compared with that from an otherwise equivalent a -Si:H specimen. To within the experimental uncertainties, there is no change. Thus a direct hyperfine coupling involving the hydrogen atoms can be ruled out for the relaxation mechanism. Furthermore, the mass of the hydrogen isotope apparently does not significantly affect any other property (e.g., phonon density of states) relevant to the dangling-bond spin relaxation. Finally, in samples with dopant concentrations varying by over a factor of 5, no variation in T_1 was observed.

The lower set of data in Fig. 6 is $T_1(T)$ for an unhydrogenated a -Si sample ($n_s \sim 10^{20} \text{ cm}^{-3}$) deposited by electron-beam evaporation. A regime of $T_1 \propto T^{-1.8}$ is found; however, the relaxation times are reduced by approximately an order of magnitude relative to the lower spin-density material. Moreover, at elevated temperatures, a lifetime reduction, due to hopping conduction between states near the Fermi level, is evident. The low-temperature data, extrapolated to lower temperatures, agree very well with data recently presented by Askew *et al.*¹⁷ for high spin density, amorphized silicon wafers. Because the quadratic behavior persists and the magnitude of T_1 is even smaller than the hydrogenated material, we infer that hydrogen plays no direct role in the two-level entities or the relaxation process.

We now show that by annealing a specimen (and driving hydrogen out) we can modify the TLS density of states of a single sample. In Fig. 7 $T_1(T)$ is plotted for an undoped amorphous silicon sample annealed for 30-min intervals at progressively higher temperatures, T_A . It is

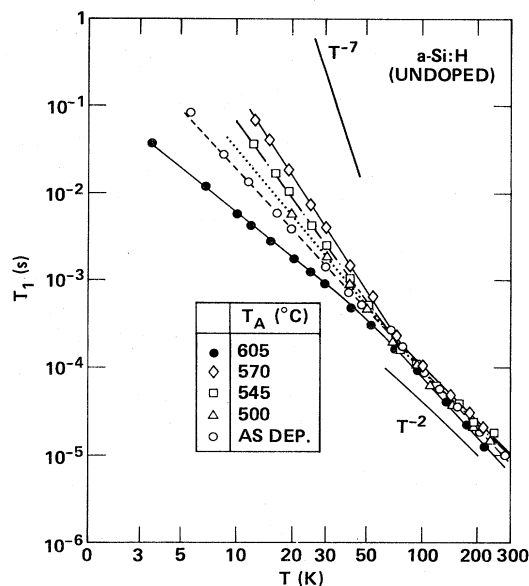


FIG. 7. $T_1(T)$ for undoped a -Si:H with the anneal temperature, T_A , as a parameter.

known that above $T_A \sim 420^\circ\text{C}$, hydrogen is evolved from these samples and the dangling-bond spin density, n_s (measured by conventional cw ESR), grows exponentially with the concentration of hydrogen removed. The rapid

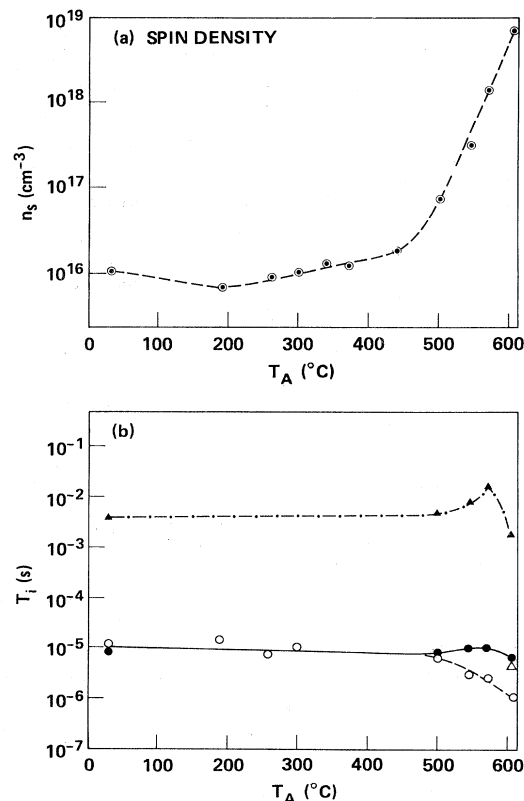


FIG. 8. Annealing behavior of (a) spin density and (b) T_1 and T_2 measured at 20 and 300 K (●, T_1 at 300 K; ▲, T_1 at 20 K; ○, T_2 at 300 K; △, T_2 at 20 K).

increase in n_s is plotted in Fig. 8(a). In Fig. 8(b) we show that for anneal temperatures above 500°C, T_2 drops and the ESR line begins to narrow due to exchange and, as shown in Fig. 7, T_1 deviates increasingly from its quadratic behavior at low temperatures. Just before the onset of crystallization (as determined by x-ray diffraction) the low-temperature dependence of T_1 drops to a $T^{-1.8}$ behavior similar to the unhydrogenated material (Fig. 6).

The increasingly superquadratic behavior of T_1 at low temperatures with hydrogen evolution seems to imply a decreasing density of TLS states at low energies with possibly a shift in the distribution to high energies. The changes correlate more directly with the increasing spin density than with the amount of hydrogen evolved. Thus the disappearance of the low-energy modes cannot be simply explained by an increase in connectivity of the network as hydrogen is removed and replaced by weak Si-Si bonds. Apparently the dangling-bond increase allows (or occurs with) the approach of the network to a thermodynamic equilibrium structure.¹⁸ The TLS density then correlates with the deviation of the network from equilibrium. (Radial distribution measurements would be useful in this regime.) Recent measurements of Raman scattering in sequentially annealed *a*-Si:H samples¹⁹ have come to this same conclusion, i.e., the amorphous network becomes more nearly ordered within ~100 K of the onset of crystallization. Narrowing and shifting of the Raman lines has tentatively been ascribed to a narrowing in the distribution of Si-Si bond angles.

Alternative and less general explanations for the increase in T_1 at low temperatures with annealing could be that the TLS correlation time may become longer for low-energy TLS, and/or the increased spin density may

saturate the TLS modes (a "TLS bottleneck") so that spin relaxation begins to occur via the usually slower two-phonon Raman channel. The decrease in T_1 (for $T_A=605^\circ\text{C}$) at high spin densities where T_2 decreases strongly is most likely due to the onset of spin diffusion. T_1 is then controlled by the fastest relaxing centers.

CONCLUSION

In conclusion, T_1 in the hydrogenated tetrahedral semiconductors *a*-Si:H and *a*-Ge:H is dominated by spin coupling to the TLS modes of the network at all temperatures up to at least 300 K. T_1 is limited by the average relaxation time of the TLS distribution. The TLS modulate the orbital angular momenta, thereby relaxing the spins via the spin-orbit interaction. The similarity of the values of T_1 (after scaling by λ^2) indicates similar network structure and excitations in *a*-Si:H and *a*-Ge:H. The small range of values for the TLS-spin coupling matrix elements would seem to follow from the relatively greater spatial extent of the TLS than the electronic states. Finally, the hydrogenated semiconductors allow one to vary the TLS density of states by annealing and to follow the related effects.

ACKNOWLEDGMENTS

We would like to acknowledge very useful discussions with B. Golding, C. Herring, R. A. Street, J. Stuke, P. C. Taylor, and G. Watkins. We would like to thank J. C. Zesch for the x-ray diffraction measurements. This work was supported in part by the Solar Energy Research Institute, Contract No. XJ-0-9079-1, and a grant from the Stiftung Volkswagen-Werk.

¹R. A. Street and D. K. Biegelsen, *Solid State Commun.* **33**, 1159 (1980).

²M. Stutzmann and J. Stuke, *Solid State Commun.* **47**, 635 (1983).

³A. Abragam, *Principles of Nuclear Magnetism* (Oxford University Press, Oxford, 1973), p. 404.

⁴W. A. Phillips, *Proc. R. Soc. London Ser. A* **319**, 565 (1970).

⁵P. W. Anderson, B. I. Halperin, and C. M. Varma, *Philos. Mag.* **25**, 1 (1972).

⁶S. Hasegawa and S. Yazaki, *Thin Solid Films* **55**, 15 (1978).

⁷R. A. Street, D. K. Biegelsen, and J. C. Zesch, *Phys. Rev. B* **25**, 4334 (1982).

⁸C. A. J. Ammerlaan and A. van der Wiel, *J. Magn. Reson.* **21**, 387 (1976).

⁹R. A. Street, J. C. Knights, and D. K. Biegelsen, *Phys. Rev. B* **18**, 1880 (1978).

¹⁰H. Dersch, J. Stuke, and J. Beichler, *Phys. Status Solidi B* **107**, 307 (1981).

¹¹J. Szeftel and H. Alloul, *J. Non-Cryst. Solids* **29**, 253 (1978).

¹²S. A. Lyon and R. J. Nemanich, *Physica* **117B-118B**, 871 (1983).

¹³B. Golding (private communication).

¹⁴B. Golding and J. E. Graebner, *Phys. Rev. Lett.* **37**, 852 (1976).

¹⁵R. C. Zeller and R. O. Pohl, *Phys. Rev. B* **4**, 2029 (1971).

¹⁶M. K. Bowman and L. Kevan, *J. Phys. Chem.* **81**, 456 (1977).

¹⁷T. R. Askew, P. J. Muench, H. J. Stapleton, and K. L. Brower, *Bull. Am. Phys. Soc.* **28**, 533 (1983).

¹⁸D. K. Biegelsen, in *Defects in Semiconductors*, edited by S. Mahajan and J. W. Corbett (Elsevier, New York, 1983), p. 75.

¹⁹R. Tsu, J. Gonzalez-Hernandez, J. Doehler, and S. R. Ovshinsky, *Solid State Commun.* **46**, 79 (1983).